Paper No. 18

ANALYSIS OF THE SIMULATION OF THE SOLAR WIND[2]

D. E. Zuccaro[1]

REFERENCE: Zuccaro, D. E., "Analysis of the Simulation of the Solar Wind," ASTM/IES/AIAA Space Simulation Conference, 14-16 September 1970.

ABSTRACT: This analysis surveys the properties of the solar wind, establishes a set of requirements for solar wind simulation, and develops a conceptual design of a simulator system. The significant features of the design are the following. The protons are formed in an r-f excited plasma discharge ion source. A 20^{o} deflection magnetic mass separator is used to purify the proton beam of other ions, energetic charge exchange neutrals, and Lyman alpha photons. The use of a small diameter beam permits differential pumping of the ion source and the sample chamber. The proton beam either can be expanded to flood the sample, or it can be scanned over the sample.

KEY WORDS: solar wind, charge exchange, charge neutralization, sputtering, proton sources, mass separators, ion optics, ultra-high vacuum systems.

I. INTRODUCTION

The development of spacecraft thermal control coatings requires the laboratory evaluation of the coating's resistance to damage induced by solar photon and particulate radiation. As the characteristics of the solar wind (or solar particulate radiation) have been determined rather recently, various types of simulators, which had different operating and performance characteristics, were fabricated. The Hughes Research Labora-

[1]Ion Device Physics Dept., Hughes Research Laboratories, Malibu, California.

[2]This work was performed under Contract NAS 2-5585.

tories has performed a study of the simulation of the solar wind for the Ames Research Center of the National Aeronautics and Space Administration. The goals of this program were to survey the properties of the solar wind, to establish the requirements for a solar wind simulator, to analyze the techniques and apparatus to be used in the system, and to establish an optimized system and its operating techniques.

This publication is one of a pair that report the results of this study. The companion paper by King[1] analyzes the ion sources, mass separators, and ion optics systems needed to form a proton beam that uniformly irradiates a 10 cm diameter sample. This paper will survey the solar wind properties, the simulator requirements and, using the results of King's analysis, establish a conceptual optimized simulation system.

II. SOLAR WIND COMPOSITION

The particle environments in space that are of principal interest to the designers of spacecraft are the solar wind and the radiation that exists at synchronous orbit. The latter has been summarized in an extensive survey by Stanley and Ryan.[2] The properties of the solar wind, which have been measured by a number of satellite probes, will be summarized in this section of this paper.

The solar wind is the term applied to the streaming plasma that is evolved from the sun. Because the energy of the particles is much greater than that which can be associated with the corona temperatures, it is believed to result from a supersonic expansion of the corona's charged particles coupled to the sun's magnetic field. The plasma is neutral, having an equal number of positive charges and electrons per unit volume. The ions and electrons have much different velocities.

The most abundant type of ion is the hydrogen ion, H^+ (i.e., a proton). The second most abundant type is the doubly charged helium ion, He^{2+} (i.e., an alpha particle). The He^{2+} to H^+ ratio (η_α/η_p) has been measured by the Vela 3A and 3B satellites.[3] During a two year period, the ratio varied over the range of 1 to 8%, with an average value of 3.7%. The variation is believed to reflect time changes in the plasma composition. During periods of solar activity, i.e., solar flares, the plasma contains a much greater He^{2+} content. In a recent class 3B flare, an η_α/η_p ratio of 0.22 was observed.[4] Under this condition nearly half the charge of the solar wind is carried by the He^{2+} ions.

---

[1] The numbers in parentheses refer to the list of references appended to this paper.

Although there are spectroscopic data indicating the presence of many other elements in the sun, only multiply charged oxygen ions O^{5+}, O^{6+}, and O^{7+} have been identified[5] at this time. The heavy ion component could be resolved only under quiet sun conditions. During this period it was about 0.5% (by number ratio) of the proton flux.[5] Other ions are believed to be present,[6] but their low relative abundance and the number of ionic states makes it very difficult to identify them by means of energy per charge detectors. The foil collector experiments made during the recent Apollo flights should provide more information about the heavy ion composition of the solar wind.

The solar wind proton energies were first accurately measured by the Mariner 2 satellite[7] in the final third of 1962. The average of the daily average proton energies for the period was 1325 eV. The 3 hour averages ranged from a low energy of 540 eV (which is associated with quiet sun conditions) to a high energy of 3100 eV. The Vela 2A and 2B satellites made about 13,000 measurements[8] during a period of minimum solar activity from July 1964 to July 1965. The mean value of the proton energy was 920 eV. The largest number of cases was for a 550 eV particle energy, which is associated with the quiet sun condition that was prevalent throughout most of the period. This distribution of proton energies is shown in Fig. 1.

The energy of the He^{2+} ions was 4 times that of the solar wind protons. The highly charged heavy ions (O^{7+}, O^{6+}, and O^{5+}), which could be resolved only during quiet sun periods,[5] had energies of about 20 times that of the protons.

The solar wind ion flux is about 2×10^{8} cm^{-2} sec^{-1} during quiet sun conditions.[6] This value is relatively constant, and its variation with solar activity generally less than a factor of 2.

The determination of the solar wind electron properties is difficult because the low energy of the electrons means the spacecraft potential can perturb the measurements and the solar induced photoelectrons can cause erroneous measurements. The most accurate measurements are the recent Vela 4B observations[9] which showed that electron energy spectrum has a broad maximum in the energy range of 20 to 40 eV.

III. SOLAR WIND SIMULATOR REQUIREMENTS

The requirements for the laboratory simulation of the solar wind are established mainly by the solar wind properties that have been summarized in the previous section. Additional factors such as the duration of the tests, the cost and com-

plexity of the equipment, the need for accelerated testing, and the size and number of samples must be considered.

A. Particle Composition

The most important parameter to be specified is that of the ion composition. All efforts to date to simulate the solar wind have used either proton beams that were purified by mass separation, or mixed (unpurified) ion beams. The latter contain molecular hydrogen ions (H_2^+ and H_3^+) as well as other ions.

Although it is possible to rule out total simulation of the solar ion plasma (H^+, He^{2+}, O^{7+}, O^{6+}, and O^{5+}) because of the prohibitively expensive and complex apparatus required to produce such a plasma, it is important to note some of the possible effects of these minor constituents. For example, the sputter yield of oxygen ions is 100 times that of protons.(10) Thus, the oxygen ion component would have about the same sputtering effect as the proton component of the solar wind. The interaction of highly charged ions, such as O^{7+}, O^{6+}, and O^{5+}, with the surface results in the formation of x-ray photons or Auger electrons. Both of these can produce secondary ionization in the target. In this case, the effect of the heavy ions is much greater than that of the protons.

Based on the present limitations, simulation of the solar wind is limited to the use of pure proton beams. Nevertheless, one of the first tasks of this optimized simulator will be to determine if the simulation of the minor constituents of the solar plasma is necessary. This could be done with a less complex O^+ or O^{2+} source in combination with an x-ray source.

B. Particle Flux

The simulation of the solar wind requires a proton flux of 2×10^8 cm^{-2} sec^{-1}, which corresponds to a ion current density of 3×10^{-11} A cm^{-2}. Because this value is based on satellite data that were obtained during a period of decreasing and minimum solar activity, it may be necessary to modify the value for the period of maximum solar activity. The change should be a small one. A much higher flux level may be required to accelerate the testing rate. This will be particularly true when radiation resistant coatings are developed. At present, accelerated testing of photon (light) induced damage is performed with 5 to 50 equivalent suns, where limitation is the output of the sources and the reciprocity failure of the samples. A proton beam of 2×10^{11} cm^{-2} sec^{-1} (ion current density of 3×10^{-8} A cm^{-2}), which corresponds to a level of 1000 times the normal solar plasma flux, is readily obtained. This is an acceptable design goal as far as the engineering aspects are con-

cerned. The operating limit may be less than 1000 times the normal plasma flux because of reciprocity failure of the sample.

C. Particle Energy

The simulator should be capable of producing a proton beam of uniform energy that can be varied over the range of 500 to 3000 eV, which corresponds to the range of solar proton energies. The mean energy of the solar protons is about 1000 eV.

The simulator also requires an electron emitter which is capable of providing sufficient electron current to the target to neutralize the proton beam charge at any proton beam operating level. Based on observations of the electrons in the solar plasma, these electrons should have energies of about 20 to 40 eV.

D. Beam Purity

A specification for the ion beam purity must take into account the nature of the impurity. For example, the molecular hydrogen ion (H_2^+), which is the major impurity, has chemical and physical effects that are quite similar to those produced by protons. Therefore, the effect of the molecular ions should scale approximately as does its concentration. A heavy ion, such as OH^+, will have a sputter yield over 100 times that of a proton of the same energy. Thus, in this case, a 1% OH^+ concentration will have an effect equal to the 99% proton component.

Another aspect of beam purity that must be specified is the presence of energetic neutrals formed by charge exchange. As the fast neutrals will have the same mass effects on the surface as ions, and because they are not registered as a current and are therefore not included in the dose measurements, it is essential that the number of charge exchange neutrals not exceed 1% of the proton flux. This factor is an important element in the selection of the mass separator system.

The beam purity requirement should specify a limit for energetic photons (Lyman α radiation) that are produced in the ion source. These photons, which are due to the excitation of hydrogen by electron bombardment, have energies of 10 to 13 eV. They can cause a very marked effect on the degradation of thermal control coatings.(11) The production of photons is negligible in the low pressure electron bombardment ion sources and pronounced in the plasma type ion sources. This factor is considered in the selection of the mass separator.

E. System Requirements

The specification of the operating pressure of the system must be set in terms of the partial pressures of the residual gases that can be present in the system. This is important because gases containing oxygen are known to cause bleaching of some of the color centers formed in the degradation of the thermal control coatings. The tolerance limits for these gases must be set to ensure that they will not interfere with the experiments.

Duplication of the vacuum conditions that exist in the interplanetary space (i.e., a random gas with a pressure of the order of 10^{-13} Torr and a directed pressure of the order of 10^{-11} Torr due to streaming from the sun[12] is unrealistically expensive. However, the results of solar wind simulation performed at 10^{-6} Torr are different from the effects of operating the same coatings in space. Experiments have been performed[13] that show marked changes in the reflectivity of thermal control coatings that are exposed to 10^{-5} Torr partial pressure of oxygen (after irradiation). This can also be shown by comparing the arrival rate of oxygen at 1×10^{-7} Torr to that at 1×10^{-14} Torr. The former will accumulate on a surface to form a monolayer in about 10 sec, while the later condition will require 3 years to form a monolayer.

The significance of this estimate is that it will be necessary to perform experiments on the irradiation of identical samples under a range of vacuum conditions to determine if the experiments are sensitive to the presence of specific gases. This is a standard procedure when operating an experiment in the presence of additional factors that can influence the results.

Because of the uncertainties in the estimation of residual gas effects on the experiments, the a priori establishment of partial pressure limits is not possible. Instead, it is necessary to set up guidelines which will result in the design of a system that has the capability to operate at pressures below the 5×10^{-7} Torr level. This will permit the establishment of these basic partial pressure parameters. In view of the fact that hydrogen will be the major gas present (due to the operation of the proton source), it is possible to set the total operating pressure limit at 5×10^{-7} Torr and to set, as a design goal, the limit on the total of all other gases at about 1×10^{-8} Torr.

In addition to controlling the sample temperature it is necessary to duplicate the condition that exists in space where none of the radiation from the surface and none of the gas desorbed from the surface is returned to the surface. The $3^{\circ}K$

black body condition of space must be simulated by cryogenic shrouds treated to have a high absorptivity.

Another design requirement is that the simulator system have a continuous operating lifetime that is greater than the test period. This could be of the order of 1000 hours. The reason is that the pressurization of the system to repair a component would cause the loss of the samples due to the bleaching of the irradiation damage. An alternative is to design a system in which the beam-forming components can be isolated from the samples by means of a high vacuum valve. This permits the pressurization of either element while maintaining the rest of the system under vacuum.

The specification of a proton beam area of 10 cm diameter is based on two considerations. This represents about the smallest area which can contain about 6 to 8 samples 2.5 cm diameter, which is the size normally used. This size beam is an upper limit for an expanded single proton beam. Thus, this system makes possible a direct comparison of the continuous beam and the intermittent rastered beam. This is important because larger samples will require the use of a rastered beam to obtain uniform irradiation.

IV. DESIGN ANALYSIS OF A SOLAR WIND SIMULATOR SYSTEM

This solar wind simulator system is based on the preceding discussion of the solar wind characteristics, the solar wind simulator requirements and on King's[1] analysis of the techniques and apparatus for proton beam formation. An outline drawing of the proposed system is shown in Fig. 2. It consists of an r-f excited plasma ion source, the ion optics system (which includes the mass separator), and the sample chamber. The discussion of the components is organized about these three basic elements.

A. Ion Source

King's analysis of proton sources indicated that the r-f ion source and the electron bombardment ion sources are the types best suited for use in a simulator system. The r-f ion source was selected for this design because it is capable of operating at the maximum ion current (1000 times the solar wind ion density) without causing an excessive gas load in the system. The r-f source also has the advantages of a long operating life and a high proton production efficiency.

If the accelerated testing was limited to less than about 50 times the solar wind level, the electron bombardment ion source could be used in the simulator system. This source is

readily adjustable over a wide range of ion currents, and produces ions with a narrow energy spread.

B. Ion Optics System

The beam extraction system is designed so that only the source is at high voltage. The beam is kept small until it reaches the last lens, to reduce aberrations in the lenses and separator and to reduce the size of the components. This also permits the beam to be rastered. The small size of the beam also means that it is possible to separate the source chamber from the main chamber with a small orifice without affecting the beam. Thus, the two chambers may be pumped separately and the large gas load from the source removed without interacting with the target. This system is shown in Fig. 3.

The ion extraction system or ion accelerator focuses the ions from the source into a beam with a divergence angle compatible with the rest of the ion optical system. It is operated in the accel/decel mode to prevent electron backstreaming and to permit adjustment of the beam voltage and thus the proton energy without affecting the field gradient at the surface of the plasma in the source from which the ions are extracted. The single small aperture provides adequate current while still acting as an effective flow impedance to reduce neutral hydrogen efflux from the discharge chamber.

The first or focusing einzel lens focuses the ion beam through the mass separator onto the aperture 4 cm from the exit plane of the magnetic sector. By adjusting the beam size at this aperture, the intensity of the beam which arrives at the target may be adjusted by a factor of 100.

The proton component is separated from the ion beam, which also contains molecular ions, by means of a 20° sector magnetic mass separator. King[1] has shown that this type of mass separator is superior to the E x B, the Bennett r-f field, and the magnetic lens types. It fulfills the two basic requirements - separation of the proton beam from both the charged and uncharged (i.e., photons, charge exchange neutrals) contaminants from the source without seriuosly defocusing the beam. King has discussed the tradeoff, between adequate separation of charged species and beam defocusing due to energy dispersion, that must be made in choosing the separator angle. The 20° sector separates the protons from the H_2^+ beam by 0.6 cm at the aperture stop located 4 cm downstream of the exit plane of the separator. The increase in diameter of the 1 mm diameter, 1000 V beam due to a 50 eV energy spread when passing through this 20° separator is less than 0.5 mm. Thus, a 2 mm aperture will pass all of the proton beam and block other charged species. This separator will nominally operate at a magnetic

field of 300 gauss and consume less than 200 W. It should not require water cooling. The final design of such a separator that is to be actually constructed should involve careful consideration of the shape of the magnet pole entrance and exit surfaces and of the magnetic gap itself, in order to minimize aberrations.

This 2 mm diameter aperture also serves to limit the flow of neutral gas molecules into the chamber. It is thus possible to differentially pump the gas that is released by the ion source and thus maintain the sample chamber at a better vacuum.

The second einzel lens controls the size of the beam at the target. It is capable of expanding the beam that passes through the aperture to 10 cm diameter at the target plane or maintaining the beam size at 0.1 cm so that it may be rastered.

As shown in the insert in Fig. 2, a set of deflection plates may be inserted between the second lens and the target to raster the beam.

The above four elements will provide a 10 cm diameter beam at the target in which no proton trajectory has an angle of more than 3^{o} with respect to the normal from the target plane.

C. Sample Chamber

The proton beam then passes through an all-metal high vacuum valve that serves to isolate the proton beam forming part of the simulator system from the sample chamber. This serves two functions:

1. to permit the samples to remain under vacuum in the event it is necessary to pressurize the ion source section,

2. to permit the ion source region to remain under vacuum and thus protected from exposure to water vapor during the loading of samples.

The sample chamber shown in Fig. 4 contains the neutralizer; the cryogenic shroud; the sample transfer arms; and the sample mounting plate (which supports the samples); and the proton, electron, and photon detection and measurement apparatus. The neutralizer consists of an electron emitter operating in an accel-decel mode that produces up to 3×10^{-6} A of 30 eV electrons. The cryogenic shroud is liquid nitrogen-cooled and is treated so as to have an absorptivity of 0.95 or larger.

The sample mounting plate is a constant temperature plate to which the samples are mechanically attached. Fluid is cir-

culated from an external reservoir to maintain the plate temperature. The plate is moved in the x-y plane by means of bellows sealed rotary motion drives in order to make possible sample transfer and to scan the proton and photon beams.

The sample transfer operates in the following manner. The plate is positioned above the z-axis transfer arm (see Fig. 4). The arm is extended to engage the sample holder, and the rotary motion then is used to unlock the sample. The sample is carried upward by moving the z-axis transfer arm, and the sample is tranferred to the y-axis sample transport arm. The y-axis transfer arm moves the sample into the integrating sphere.

D. Beam Measurement Apparatus

The sample mounting plate also supports the apparatus for determining the flux, energy, and profile of the proton and electron beams and the flux and profile of the photon beam. These detectors, as well as some pressure sensors, are part of the control loop that regulates the operation of the ion source and the neutralizer.

The determination of the flux, energy, and density profile of the proton beam is accomplished by use of a Faraday collector located below the sample mounting plate. The collector should have a length-to-diameter ratio of about 4 to 1 to ensure that the potential within the collector is very small and thus prevents the loss of secondary electrons or ions. Shielding and operation of the collector at a small positive bias may be necessary to prevent errors due to photoelectron currents that can result from the solar photon radiation simulation.

The proton energy is determined by measuring the beam potential as a function of bias potential on the collector. The proton beam energy spread is determined by plotting the first derivative of the beam current as a function of proton beam energy. The proton beam density profile is determined by measuring the beam flux (at a fixed set of operating conditions) at a number of points by moving the mounting plate in the x-y plane. Simultaneous measurement of the proton and electron beams is needed to regulate the operation of both sources, to provide a measurement of the proton dose rate during the run, and to verify the degree of neutralization. This can be accomplished by passing the combined beam (protons and electrons) through an aligned electric and magnetic field. The electrons are swept out by fields to another collector, thus giving an electron and an ion current.

Some of the experimental problems that should be anticipated in the design of the measurement apparatus include both extremely low signal levels and the high noise levels that can

result from the r-f generator used in the ion source, the plasma in the ion source, stray electron currents in the chamber, and photoelectrons. While there is little that can be done about the low signal levels (e.g., signal of the order of 10^{-12} A), there are a number of remedies for the high noise level. The r-f and plasma noise can be reduced by the use of π or T section filters or by the use of ferrite beads. The design of the filters can be obtained from any standard text. Carefully designed shields are the most effective way of preventing the stray electron currents from measurement as part of the signal. Photoelectric currents can be suppressed by operating the collector at a slightly positive bias with respect to the surroundings.

The ion-electron converter[14],[15] can be used for visual check of the beam shape and density variations. This consists of a fine metal mesh mounted near an electron excited phosphor on a plate. The ions strike the mesh, generating secondary electrons that are attracted to the phosphor, which is held at a high positive potential. Use of an electroformed nickel mesh of 400 wires cm^{-1} gives resolution on the order of 25 to 50 μm.

E. Vacuum Pumps

The vacuum pumps shown in Fig. 2 consist of two pairs of sputter ion and titanium sublimation pumps. The combination is necessary because the pumping mechanism for hydrogen in a sputter ion pump is limited to chemical reaction (gettering) with the cathode material.[16],[17] The titanium sublimation pump is added to increase the pumping of the hydrogen (as well as any other chemically reactive gases). The sputter pump must handle the gases that are not gettered by the titanium.

The use of liquid helium cooled cryogenic pumps is not advisable for a system in which the predominant gas load is hydrogen. The reason is that the vapor pressure of hydrogen is of the order of 10^{-6} Torr at a cryopump temperature of the order of 4.5 to 4.2°K.[18] This value is poorer than that which can be obtained from the TSP and ion pump.

V. SUMMARY

The design that has been produced satisfies the requirements for simulation of the solar wind. The most significant features are:

a. the magnetic mass separator to purify the beam of other ions, energetic charge exchange neutrals, and Lyman alpha photons,

b. the small ion beam that makes possible differential pumping of the system,

c. the direct comparison of the expanded versus the scanned beam, and

d. the isolation valve between the beam forming system and the sample chamber.

VI. REFERENCES

1. H. J. King, "Solar Wind Simulator, to be given at Space Simulation Conference, 14-15 September 1970, Gaithersburg, Maryland.

2. A. G. Stanley and J. L. Ryan, "Charged Particle Radiation Environment in Synchronous Orbit," Technical Report 443, Contract AF 19 (628)-5167, MIT Lincoln Laboratory, 15 May 1968.

3. D. E. Robbins, A. T. Hundhausen and S. J. Bame, J. Geophys Res. 75 , 1178, (1970).

4. J. Hirshberg, A. Alksne, D. S. Colburn, S. J. Bame, and A. J. Hundhausen, J. Geophys Res. 75 , 1 (1970).

5. S. J. Bame, A. J. Hundhausen, J. R. Asbridge, and I. B. Strong, Phys. Rev. Letters 20 , 393 (1968).

6. A. J. Hundhausen, Space Sci. Rev. 8 , 690 (1968).

7. M. Neugebauer and C. W. Snyder, J. Geophys. Res. 71 , 4469 (1966).

8. I. B. Strong, J. R. Asbridge, S. J. Bame, and A. J. Hundhauser, in "Zodiacal Light and Interplanetary Medium," J. Winberg, Ed., NASA SP-150, 1967.

9. M. D. Montgomery, A. J. Bame, and A. J. Hundhausen, J. Geophys. Res. 73 , 4999, (1968).

10. F. Grønlund and W. J. Moore, J. Chem. Phys. 31 , 1132 (1959).

11. D. D. Swofford, V. L. Mangold, and S. W. Johnson, Thermal Design Principles of Spacecraft and Entry Bodies, J. T. Bevans, Ed. (Academic Press, New York, 1968),p.667.

12. L. A. Nelson, Handbook of Solar Simulation for Thermal Vacuum Testing , J. S. Griffith, Ed. (Institute for Environmental Sciences, 1968). p.3-1.

13. J. E. Gilligan and G. A. Zerlant, AIAA Paper No. 69-1025, AIAA/ASTM/IES 4th Space Simulation Conf., Los Angeles, 8-10, September 1969.

14. G. Kuskevics, J. Appl. Phys. 39 , 4076 (1968).

15. D. M. Jamba and O. Husmann, J. Appl. Phys. 38 , 2630 (1967).

16. S. L. Rutherford and R. L. Jepsen, Rev. Sci. Instr. 32, 1144 (1961).

17. S. L. Rutherford, S. L. Mercer, and R. L. Jepsen, 1960 Seventh National Symposium on Vacuum (Pergamon Press, New York, 1961).

18. E. S. Borovik, S. F. Grishin, and Ya. Grishina, Soviet Phys. Tech. Phys. 5 , 505 (1960).

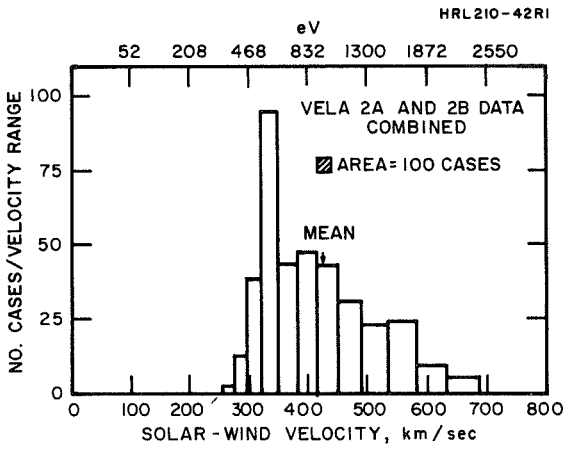

Fig. 1. Distribution of solar-wind ion energy and velocity from July 1964 to July 1965 (from ref. 8).

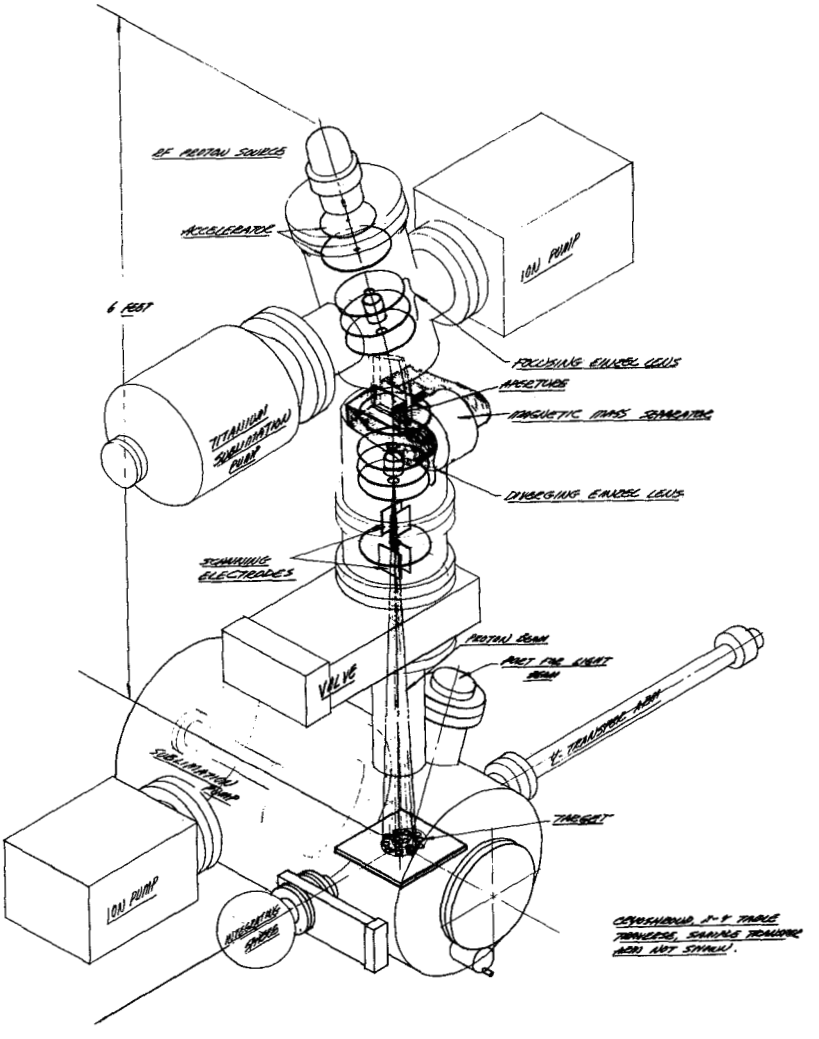

Fig. 2. Solar wind simulator system.

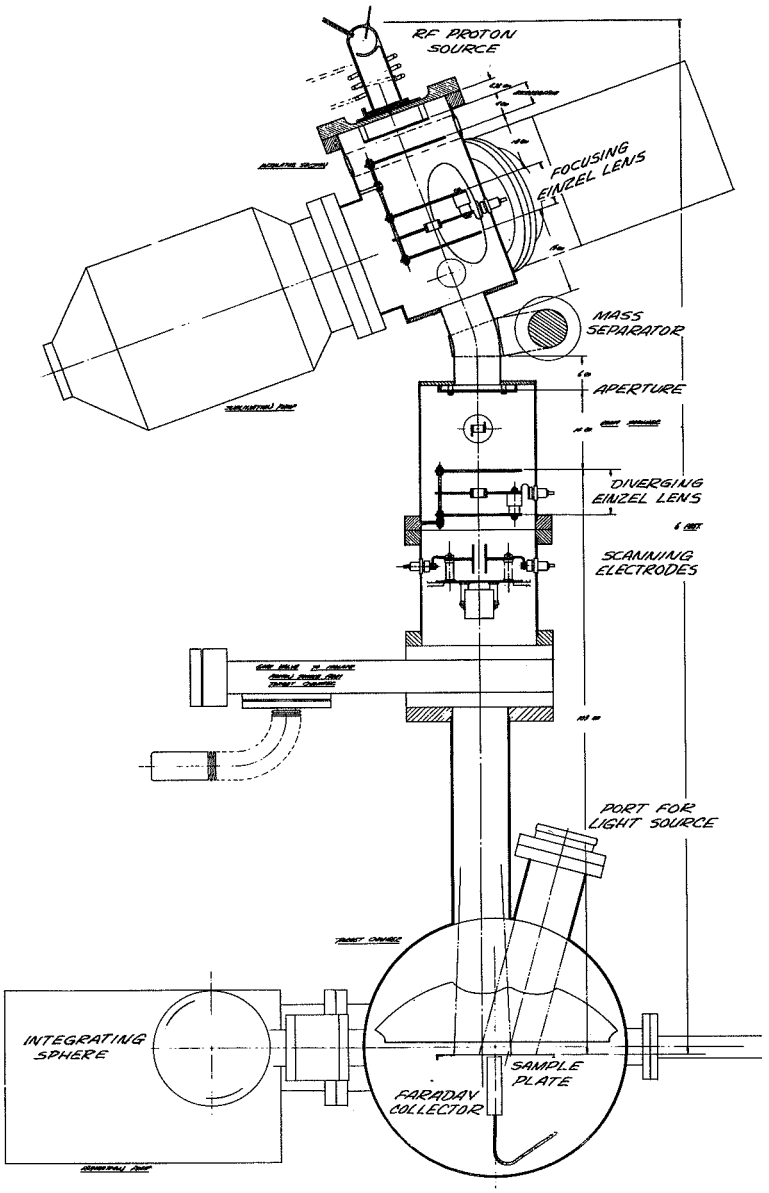

Fig. 3. Layout of solar wind simulator.

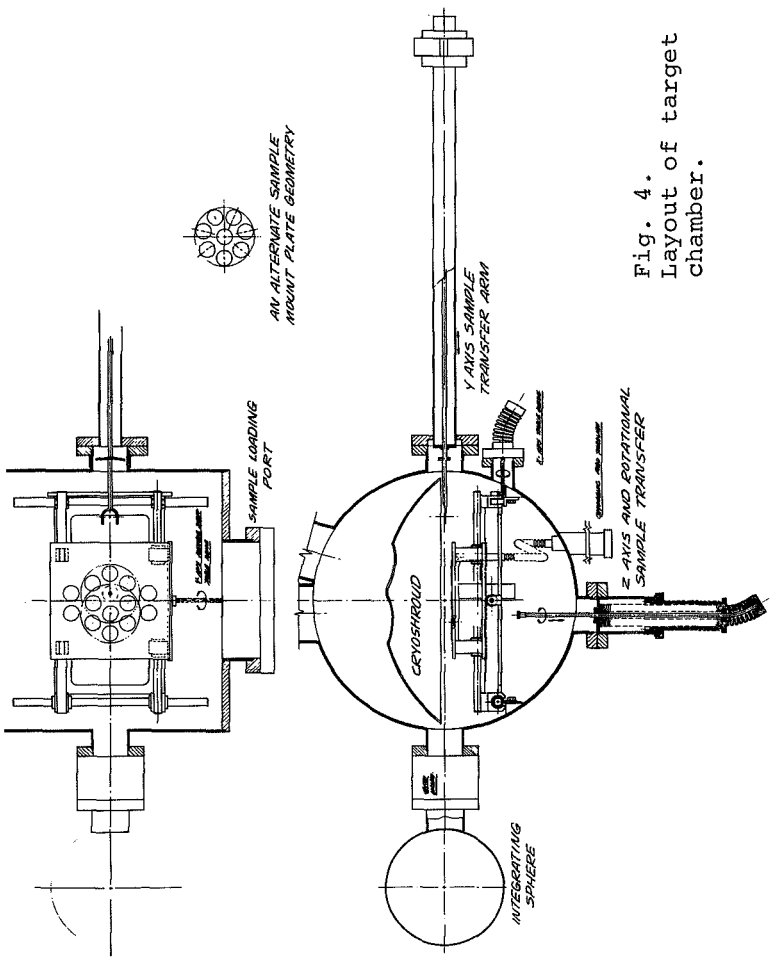

Fig. 4.
Layout of target chamber.